



Systematic design methodology and construction of UAV helicopters[☆]

Guowei Cai, Lin Feng, Ben M. Chen^{*}, Tong H. Lee

Department of Electrical and Computer Engineering, National University of Singapore, Singapore 117576, Singapore

ARTICLE INFO

Article history:

Received 28 November 2007

Accepted 29 May 2008

Keywords:

UAV helicopters

Virtual design environment

Anti-vibration

Hardware construction

ABSTRACT

In this paper, we present a comprehensive design methodology for constructing small-scale UAV helicopters. The systematic design procedure, which includes hardware component selection, design and integration, as well as experimental evaluation, is utilized to construct a fully functional UAV helicopter, named SheLion. Various ground and flight tests have been performed to verify the feasibility and reliability of SheLion. This simple, systematic and effective methodology can be easily followed and used for building small-scale UAV helicopters for general research purposes.

© 2008 Elsevier Ltd. All rights reserved.

1. Introduction

Unmanned aerial vehicles (UAVs) have become a hot research topic in the last decade worldwide. Their great potential has been explored in numerous military and civil implementations. Among various UAVs, small-scale UAV helicopter is especially attractive to the academic circle due to its small size, unique flight capacities, outstanding maneuverability and low cost. Many research groups have constructed their own UAV helicopters for their research purposes (see, for example [4,6,13–15,17]). Success has been achieved in many research areas such as software design and integration (see, for example [5,22]), modeling identification (see, for example, [10,13,19,21]), control techniques implementation (see, for example [9,20]), aerial image processing (see, for example [3,11,12,17,18]), to name a few.

Designing a small-scale UAV helicopter is a challenging job, especially to the researchers with insufficient background knowledge on aerodynamics and mechanics of rotorcraft. Problems may come from various aspects such as hardware components selection, software design and anti-vibration solution. Furthermore, the commonly adopted radio-controlled (RC) hobby helicopter has strictly limited payload (less than 6 kg), which imposes much more difficulty on the design process. Although some small-scale UAV platforms have been successfully built up and implemented, there is no uniform, time-saving and effective design methodology that has been clearly documented in the literature.

Our UAV research team has recently constructed two small-scale UAV helicopters for our research purposes in implementing advanced nonlinear flight control law and tracking ground targets. The first UAV helicopter, called HeLion [1], has been successfully implemented to verify the superiority of proposed nonlinear control method, that is, the composite nonlinear feedback (CNF) control, in near hover [2] and full envelope flight [16]. Although the design and debugging procedure was pretty lengthy (one whole year) with two researchers involved, we have accumulated rich experiences and managed to summarize a simple, systematic and effective design methodology of constructing small-scale UAV helicopter with minimum complexity and time cost. Such methodology includes four steps: (1) virtual design environment selection; (2) hardware component selection; (3) comprehensive design and integration; and (4) ground and flight test evaluation. Based on this procedure, we construct our second UAV helicopter, SheLion. Compared to its counterpart, HeLion, SheLion is lighter in weight with more compact and systematic hardware layout design and more functions such as onboard image processing. Furthermore, the whole constructing period including design, assembling, debugging and testing is greatly shorten to three months with the same manpower involved.

The outline of this paper is as follows: Following the logical order of the construction of SheLion, in Section 2, we first introduce the virtual design environment, SolidWorks, which is used for building up the virtual layout of SheLion. In Section 3, the hardware components and the reasons for their selection are presented. In Section 4, the comprehensive design procedure including onboard layout design, anti-vibration design and power supply design is described. The ground and flight test results are given in Section 5 to evaluate the working performance and reliability of SheLion. Finally, in Section 6, we draw our concluding remarks.

[☆] This work is supported by the Defence Science and Technology Agency (DSTA) of Singapore under the 2003 Temasek Young Investigator Award.

^{*} Corresponding author. Tel.: +65 6516 2289; fax: +65 6779 1103.

E-mail addresses: caiguowei@nus.edu.sg (G. Cai), g0500067@nus.edu.sg (L. Feng), bmchen@nus.edu.sg (B.M. Chen), eleleeth@nus.edu.sg (T.H. Lee).

2. Virtual design environment

The first step for constructing the UAV helicopter, SheLion, is to choose a suitable virtual design environment. The design procedure in the construction of HeLion was mainly based on two-dimensional computer-aided-design (2D CAD) blueprints. The lack of a powerful 3D design environment caused great difficulty in layout design and the integration of hardware components. As a result the design and integration procedure was iterated for quite a number of times, which had prolonged the total constructing time for months. To avoid such a problem, in constructing SheLion, we employ a powerful virtual design environment, SolidWorks, which has the following main advantages:

1. *Easy to use:* Users can be familiar with the necessary functions in a short time through learning several key examples.
2. *Powerful 3D and 2D design:* In SolidWorks, the virtual counterpart can be modeled to be identical with the real hardware component, both in shape and color. When the 3D design is finished, the corresponding 2D views will be generated at the same time for the convenience of mechanical manufacturing.
3. *Physical description:* Each virtual component can be parameterized with necessary physical parameters such as density and weight. The center of gravity (CG) can be either calculated by SolidWorks or arbitrarily specified. Such a function is especially useful in the layout design of the onboard computer system of the UAV.
4. *Animation function:* For certain components, which can move or rotate, we can emulate their motions by using an animation function. This function is essential when some complicated devices, such as a two-degree-of-freedom camera frame, are needed to be mounted onboard.

Such a software-facilitated design concept is one of the most remarkable features of our proposed UAV design methodology and is closely followed throughout in the design procedure given



Fig. 1. SheLion and its virtual counterpart.

in this work. The outline of this paper is as follows: In Section 3, we present the hardware selection of the UAV helicopter systems and the construction of their virtual counterparts. Each virtual counterpart is characterized with (1) the location and dimension of its mounting hole; (2) the center of gravity; (3) the dimension of the object; and (4) its weight, which are to be specified for further development such as layout design and integration. In Section 4, each of the design steps is to be tuned virtually till it is fully determined. The virtually constructed UAV and its real counterpart are displayed in Fig. 1. It is noted that the SheLion is carefully built up in the virtual design environment, which provides an excellent backup of our design process. Through using such a software-facilitated design procedure, we have successfully avoided unnecessary iterations and greatly shortened the design period.

3. Hardware components selection for SheLion UAV helicopter

Our SheLion UAV helicopter system, whose working principle is shown in Fig. 2, is composed of the following four parts: (1) a radio-controlled (RC) bare helicopter; (2) an onboard computer system; (3) a manual control system; and (4) a ground supporting system. Among them, the RC helicopter is the baseline to be upgraded. The onboard computer system is the most important part, in charge of collecting necessary in-flight data, such as helicopter states, main rotor's RPM (rotations per minute), sonar-measured altitude and servo actuator deflection, and onboard images, analyzing the data and images collected, and implementing flight control laws as well as logging data to the compact flash (CF) memory cards. Each of the solid block in Fig. 2 represents a specific hardware component and their functions and selections are to be presented in detail in Sections 3.1–3.6 and 3.7. The manual control system, which is normally a radio-controlled joystick, always comes with the RC helicopter and is used to control the helicopter by the pilot in manual flight tests. Lastly, the ground supporting system is used to monitor the flight status of the UAV helicopter online and to communicate with the onboard computer system. From Fig. 2 it can be noted that building a UAV helicopter is heavily related to hardware components selected. In what follows, we present the selection of necessary hardware components for SheLion.

3.1. RC helicopter

A high quality RC bare helicopter, Raptor 90, is selected as the basic rotorcraft of SheLion. It is shown in Fig. 3 along with its virtual counterpart. Some key physical parameters of the helicopter are listed in Table 1. Five onboard servo actuators are used to drive the helicopter. More specifically, the aileron, elevator and collective pitch servos are in charge of tilting the swash plate to realize the rolling motion, pitching motion and to change the main rotor's collective pitch angle. The throttle servo, cooperated with a hobby-purpose RPM governor, is used to control the engine power. One high-speed digital servo, associated by a low cost yaw rate gyro, is employed to control the yaw motion. The commonly used stabilizer bar, which acts as a damper to reduce the over-sensitive aerodynamic forces caused by the ultra small size of helicopter, is also equipped to facilitate manual control. The Raptor 90 helicopter is well suited to our UAV helicopter's upgrading because of the following three reasons:

1. *Great maneuverability:* Raptor 90 helicopter is originally designed for F-3D acrobatic flight. Its agility and maneuverability are both famous in the RC hobby flight circle. Correspondingly the upgraded UAV helicopter holds more control flexibility compared with those upgraded from RC helicopters developed for F-3C stable flight.

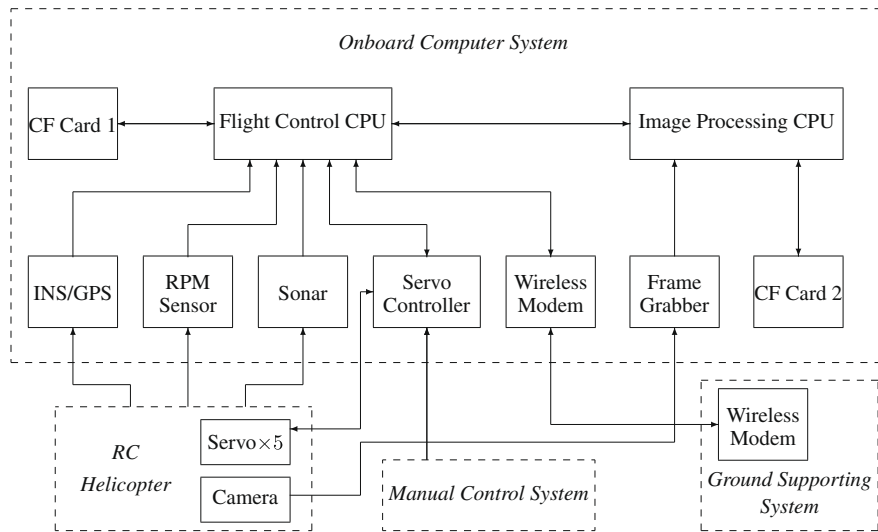


Fig. 2. Working principle of the Shelion UAV helicopter system.



Fig. 3. Raptor 90 RC helicopter and its virtual counterpart.

Table 1
Specifications of Raptor 90 helicopter

Specifications	Raptor 90 helicopter
Full length of fuselage	1410 mm
Full width of fuselage	190 mm
Main rotor diameter	1605 mm
Tail rotor diameter	260 mm
Weight	4900 g
Maximum flight time	12 min

- Large payload:** The equipped OS-91SX engine is capable of generating 3.1 ps at 15,000 rpm, resulting in the maximum taking-off weight up to 11 kg. Since the dry weight of helicopter is about 4.9 kg, the effective payload is up to 6 kg, which suits well with our budget of the weight (i.e., 3.5 kg) for the onboard computer system and provides sufficient room for future upgrading.
- Low cost but high performance:** Compared with other expensive but same size RC helicopters such as Hirobo-90 and Bergen Industrial Twin, Raptor 90 helicopter provides the same high quality flight performance but at a half price.

3.2. Computer processor boards

For the selection of computer processor boards, we adopt PC-104 standard processor boards because of the following three fea-

tures: (1) the small but uniform size (96 mm × 90 mm × 10 mm); (2) light weight (normally less than 200 g); and (3) anti-vibration structural design (pin-and-socket bus connection method). The most challenging issue we are facing is to ensure the working efficiency while strictly avoiding computational overloading and software crash during actual flight tests. Unlike the onboard system adopted in our previous UAV, HeLion, SheLion has an onboard image processing unit to carry out real-time process of images captured by the onboard camera. As such, we separate the onboard system into two parts and employ two processor boards, of which one, called the *flight control CPU*, is in charge of all of flight control missions, and the other, called the *image processing CPU*, is particularly used for image processing. By doing so, the image processing function, which is both time and computational resources consuming, is completely isolated from the missions related to automatic flight control and thus the overall safety of the onboard computer system is not affected.

The main tasks of the flight control CPU (see Fig. 2) are: (1) collecting data from INS/GPS and RPM sensors, sonar and servo controllers; (2) analyzing collected data; (3) implementing flight control laws and driving servo actuators through servo controllers; (4) logging the in-flight data to CF Card 1 for post-flight analysis; (5) communicating with the image processing CPU; and (6) communicating with the ground supporting system. Although there are multiple flight missions involved, it has been proved in [5] that the computational load for normal flight tests is fairly light (less

than 23% in the CPU usage at the peak) for a 600 MHz CPU board used in HeLion. Consideration for the selection of the flight control CPU for SheLion is more on reducing the weight and power consumption while maintaining the system safety and working efficiency. We choose a PC-104 ATHENA, which has four RS-232 serial ports, a 16-pin digital-to-analog (D/A) port, two counters/timers and runs at 600 MHz. PC-104 ATHENA is a 3-IN-1 board, which integrates all of the necessary functions of a main processor board, a serial communication board used for data exchange with INS/GPS, servo controller and wireless modem, and a data acquisition board used for data exchange with RPM sensor. As a result the weight and power consumption are greatly reduced to 30% and 50%, respectively.

The image processing CPU, is only assigned tasks related to on-board image processing, which include: (1) collecting ground images; (2) analyzing image data for ground target detecting and tracking; and (3) communicating with the flight control CPU. Since the image processing job requires large amount of computational resources, a high-speed PC-104 board running at 1 GHz, namely, CRR-III, is selected. One PC-104 standard frame grabber card is attached to the CRR-III for the purpose of A/D conversion and transformation of collected images.

3.3. Avionic sensors

There are three key avionic sensors equipped on SheLion: (1) an INS/GPS measuring all of the necessary helicopter states; (2) an ultrasonic sonar measuring the altitude in the near ground level; and (3) an RPM sensor recording the RPM of the main rotor. Their selections are based on the following.

The core navigation sensor, i.e., INS/GPS, is selected in accordance with the requirements on its output signals:

1. The essential signals that the INS/GPS is to provide are three-axis angular rates, three-axis accelerations, three-axis magnetics and three-axis positions. The first three are in body frame of the UAV and the last one resides in the NED (north-east-down) frame. It is noted that the three axis Euler angles are not necessary since they can be estimated by using an extended Kalman filter (EKF) as reported in [8] and complementary filtering reported in [23].
2. The measuring ranges of the three-axis accelerations, three-axis angular rates and three-axis magnetics are set as ± 2 g, $\pm 150^\circ$ and ± 0.7 Gauss, respectively, in accordance with the specifications of the commonly used commercial products. The selected threshold values are reasonable since we do not intend to cover the extreme or acrobatic flight conditions. As a result, the accel-

eration, angular rate and magnetics are not to change dramatically during flight tests. Based on this setting, we need to carefully perform an anti-vibration design to avoid the measurement saturation caused by various vibration sources associated with the UAV. This is to be addressed in Section 4.2.

3. On the basis of meeting all of above mentioned requirements, the size, weight and power consumption of newly adopted INS/GPS should be minimized.

A compact INS/GPS, namely, MNAV100CA, shown in Fig. 4 along with the virtual counterpart, is selected for SheLion. The key specifications of this sensor are listed in Table 2, which clearly shows that all of the requirements are satisfied. Furthermore, by using MNAV100CA, the weight and power consumption of the INS/GPS sensor are greatly reduced to 5.6% and 16%, respectively, compared to those of the fully integrated INS/GPS, NAV420CA, installed on HeLion. It is to be verified in Section 5.2 by various flight tests that the compact INS/GPS yields the similar level of working performance as the expensive one adopted in HeLion.

The ultrasonic sonar is capable of providing altitude signal in near ground level. Due to the inaccuracy of the GPS signals, the altitude signal generated by the sonar is the key reference for automatic taking-off and landing processes. SheLion adopts an ultrasonic sonar, namely, SNT-UPK2500, with a resolution in the mm range and a weight of 50 g. The effective range is up to 2 m, which is sufficient for automatic taking-off and landing.

The RPM sensor, Futaba GV-1, is a commercial product which is commonly used in the RC hobby flight circle. To simplify the overall design, we retain this product in SheLion but with necessary modifications to obtain the RPM number, which is originally set as an internal signal. More specifically, we connect the RPM sensor to a Schmidt Trigger and the output of the Schmidt Trigger is then sent to a counter/timer port resided in PC-104 ATHENA processor board.

Table 2
Specifications of MNAV100CA

	Requirements	MNAV100CA
Acceleration range X/Y/Z (g)	± 2	± 2
Angular rate range ($^\circ$)	± 150	± 200
Magnetometer range (G)	± 0.7	± 0.75
GPS accuracy in CEP (m)	≤ 3	3
Update rate (Hz)	≥ 50	1–100 programmable
Size (mm)	$\leq 76 \times 97 \times 76$	$57 \times 45 \times 11$
Weight (g)	≤ 580	33
Power consumption (W)	≤ 5	≤ 0.8

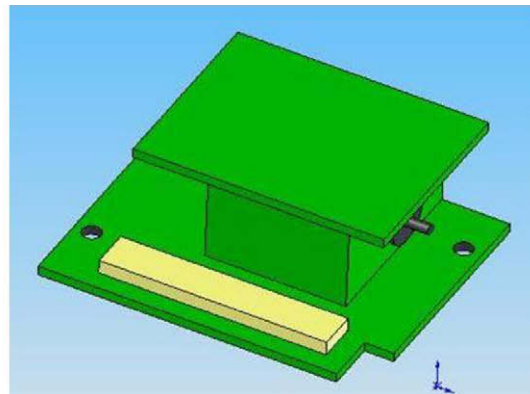


Fig. 4. MNAV100CA and its virtual counterpart.

3.4. Servo controller

Servo controller is used to realize smooth switching between the manual control mode and automatic control mode. The requirements for the servo controller are listed as follows:

1. *Reliable switching function*: The switching between automatic control and manual control should be both fast and smooth. A particular channel must be assigned to ensure the reliability.
2. *Sufficient input/output channels*: For most RC helicopters, five onboard servos are equipped to drive the helicopter. Adding an extra channel for switching function and some necessary redundancy, the input/output number must not be less than 7.
3. *Capacity of recording servo actuator's input signal*: This function is particularly important in initial manual flight tests. The recorded input data are essential for deriving the dynamical model of the UAV and for evaluating control performance.
4. *High resolution*: Substantially the input-recording and servo-driving function are the A/D and D/A procedure. The resolution should be sufficiently high to ensure the data consistency and accuracy.

The final selection of the servo controller, an HBC-101, is an 8-input/8-output digital signal processing (DSP) board with a resolution of 0.009°. RS-232 serial protocol is used to exchange data with PC-104 ATHENA. Input channels 2–6 and serial port are assigned to receive the manual input signals and ATHENA-generated auto input signals, respectively. Channels 7 and 8 are currently not in use. Lastly, Channel 1 is preoccupied by the switching function. The switching signal comes from the manual control joystick. By doing so the pilot owns the highest authority to determine which side (automatic or manual input) is mapped to the output. Such a *piloted-highest-control* design is especially important during some unexpected situations since the pilot can immediately retrieve back the manual control to avoid accident or crash.

3.5. Camera and laser pointer

A camera and laser pointer are equipped onboard for ground target tracking. The camera is for collecting images of ground targets and transferring back to the frame grabber for further processing. The main consideration for its selection is making a suitable trade-off between the resolution and the weight and volume of the camera. A compact CMOS camera with ultra small-size (25 × 25 × 30 mm), light weight (10 g) and acceptable resolution (640 × 480 pixels), is chosen for SheLion. The laser pointer acts as the emulation of a machine gun for attacking ground targets. For our research purpose, a commercial low-cost laser pointer with a weight of 15 g is selected. Its effective range is 40 m.

3.6. Wireless modem

The wireless communication between SheLion and the ground supporting system is realized by a pair of serial wireless radio modems (one installed on the UAV and the other on the ground supporting system). We select Freewave IM-500 wireless modem system with a light weight (75 g), high throughput (115.2 kbps), wide range (up to 32 km in the open field environment) and a working frequency at 2.4 GHz.

3.7. Onboard battery

Four WorleyParsons lithium–polymer batteries are used to provide electrical power to both the onboard computer system and the onboard servo actuators. Compared with other types of batteries such as Ni–Mh batteries, Ni–Cd batteries and Li–ion batteries, lith-

Table 3

Key hardware components adopted by SheLion and HeLion

Components	SheLion	HeLion
Flight control CPU	ATHENA (600 MHz, 3-IN-1)	CRR-III 650 (650 MHz)
Serial Board	N/A	OPTO-104 (four serial ports)
Data acquisition board	N/A	DMM-32X-AT (32 A/D inputs)
Image Processing CPU	CRR-III 1G (1 GHz)	N/A
Frame grabber	Colory-104 (four video channels)	N/A
INS/GPS	MNAV100CA	NAV420CA
Ultrasonic sonar	SNT-UPK2500 (2 m range)	SNT-UPK2500 (2 m range)
RPM sensor	Futaba GV-1	Futaba GV-1
Servo controller	HBC-101 (8-in/8-out)	HBC-101 (8-in/8-out)
Wireless modem	Freewave IM-500 (32 km range)	Freewave IM-500 (32 km range)
Onboard batteries	WorleyParsons Li-Po (8.4 V/35 W) × 2	WorleyParsons Li-Po (8.4 V/35 W) × 2

ium–polymer batteries have the advantage of having higher power capacity, less memory effect and lighter weight. The capacity of selected batteries is to be discussed latter in Section 4.3.

Finally, to conclude, we summarize in Table 3 the key components and their specifications adopted by SheLion and its counterpart, HeLion, for easy reference and comparison.

4. Systematic integration of SheLion onboard system

Based on the hardware components selected in Section 3, we now proceed to carry out a systematic integration of those components for the SheLion onboard system. The procedure consists of four parts: (1) the onboard layout design; (2) the anti-vibration design; (3) the power supply design; and lastly (4) electromagnetic interference (EMI) shielding design.

4.1. Onboard layout design

Layout design for onboard computer systems is a challenging issue for small-scale UAV helicopters. There is no systematic methods reported in the literature to date. In what follows, we aim to propose a simple and uniform layout design approach, which can be easily followed and adopted to construct small-scale UAV helicopters. The procedure is independent of hardware components used. The proposed approach includes the following four steps (see Fig. 5; interested readers are referred to a video clip linked at <http://hdd.ece.nus.edu.sg/~uav/wmv/3DVirtualDesign.wmv> for graphical illustration):

Step 1: Determining the location of INS/GPS. The essential rule of this step is to mount the INS/GPS as close as possible to the CG of the UAV helicopter to minimize the so-called *lever effect*, which can cause bias on the measured accelerations when the UAV performs rotatory motions. Based on the experience we gained from the construction of our earlier version UAV, HeLion, we find that it is easier to control the UAV when the onboard system is mounted underneath the bare helicopter. For such a layout, the general guideline is to line up the CGs of the INS/GPS, the onboard computer system and the basic helicopter along the z-axis of the body frame. Since the CG location of the bare helicopter is fully known using pendulum test introduced in [7], the mounting location of the INS/GPS in x–y plane of body frame can be determined. The offset between the CG of the UAV helicopter and that of the INS/GPS is only in z-axis and unavoidable. However, it can be minimized by

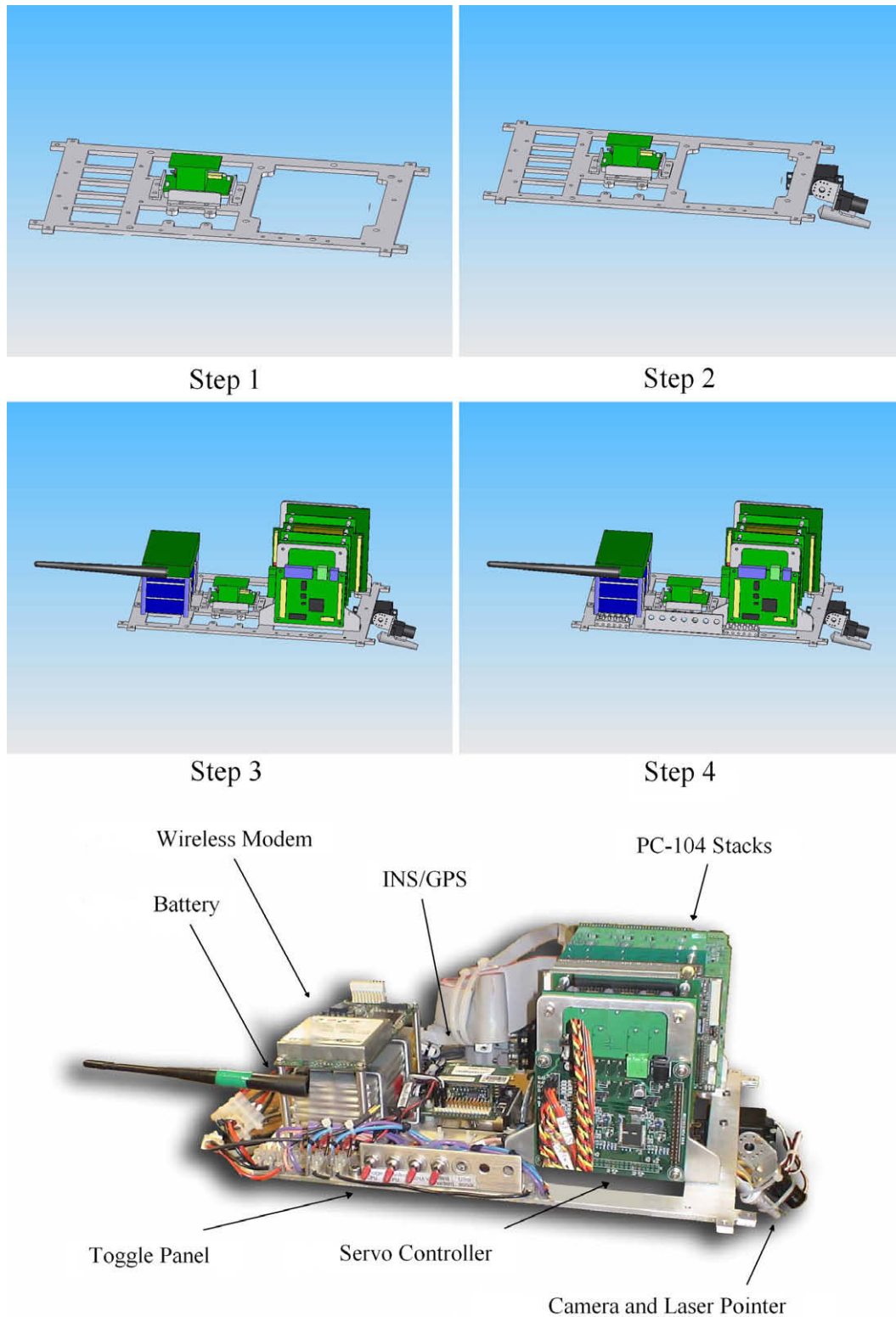


Fig. 5. Layout design procedure and the final onboard system.

carefully considering the height of onboard system and adding necessary space between the bare helicopter and the onboard system for bumping avoidance.

Step 2: Determining the location of the camera and laser pointer. The onboard camera and laser pointer are employed for ground target tracking and attacking, their mounting locations should have a good eyesight and sufficient moving space.

To fulfill these requirements, they are both mounted at the most front part of the onboard system. To simplify the design, these two components are bound with each other in parallel and attached to a digital servo, which is capable of providing motion in pitch direction. In searching or attacking a ground target, the yaw direction movement is to be controlled and accomplished by the UAV itself.

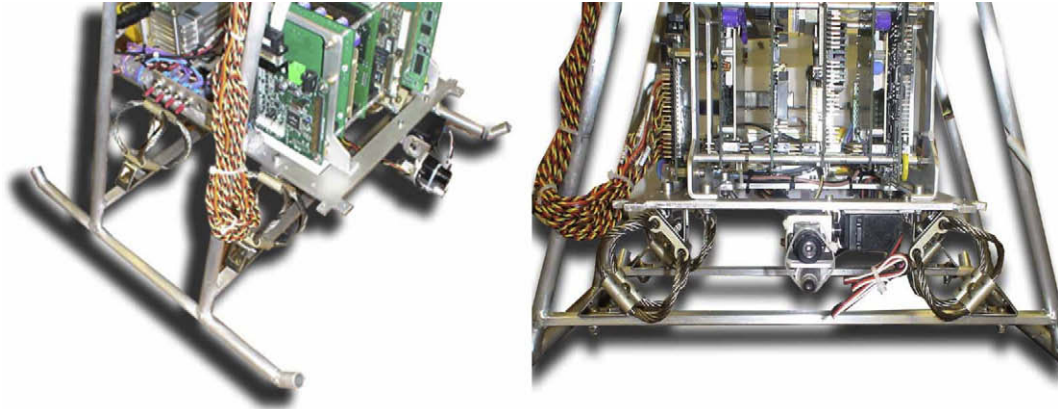


Fig. 6. Anti-vibration design for the onboard computer system (left, side view; right, front view).

Step 3: CG balancing. The locations of the following four components, i.e., the two PC-104 processor boards, the servo controller, the wireless modem, and the battery packs, have also to be carefully selected. In general, the PC-104 processor boards and servo controller board are to be mounted at the front part for the convenience of cable/wire connection and the wireless modem is mounted on the back for the ease of wireless communications. The battery packs are also placed on the back to balance the overall CG of the onboard system. Furthermore, we also guarantee that the CG of the onboard system coincides with the CG of the INS/GPS, and the onboard system is symmetrical in both longitudinal and lateral directions.

Step 4: Locating the remaining light-weight components. The remaining light-weight (less than 50 g) components include ultrasonic sonar and toggle panel, for which anti-pollution and short circuit avoidance are the main consid-

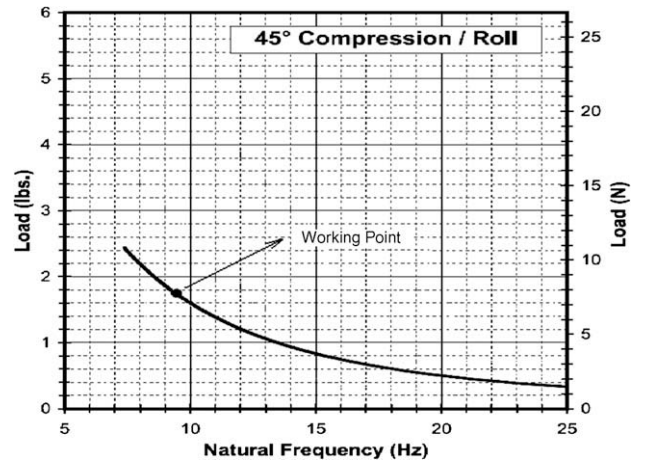


Fig. 7. Working point of the selected wire-rope isolators.

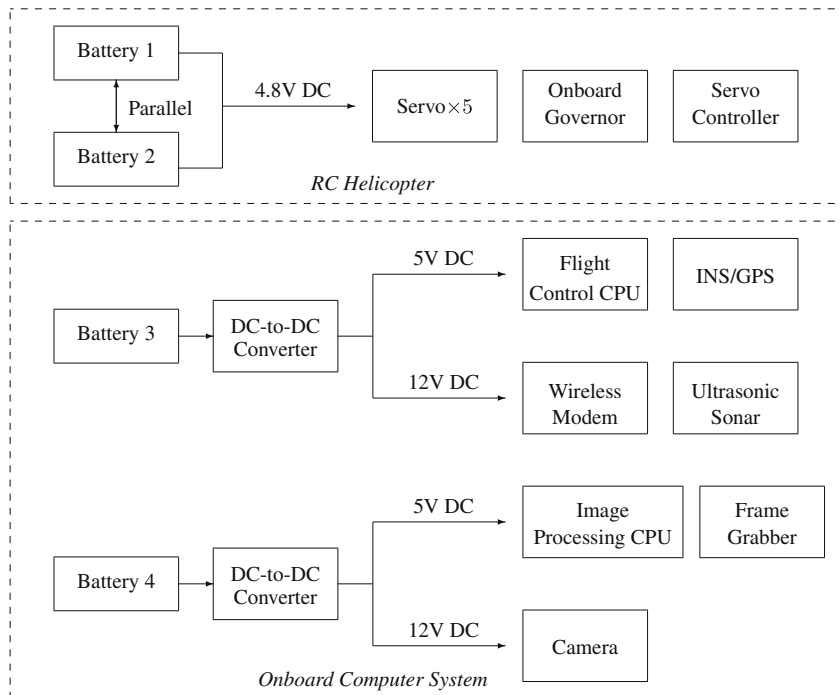


Fig. 8. Power supply design for SheLion UAV helicopter.

Table 4
Power consumption list for SheLion UAV helicopter

Hardware component	Power consumption (W)
Flight control CPU	12.5 (at 5 V DC)
INS/GPS	0.5 (at 5 V DC)
Servo controller	1 (at 5 V DC)
Wireless modem	3.9 (at 12 V DC)
Ultrasonic sonar	1 (at 12 V DC)
Image processing CPU	19.5 (at 5 V DC)
Frame grabber	0.5 (at 5 V DC)
CMOS camera	0.6 (at 12 V DC)

eration. At the end, we decide to place the sonar on the landing skit and the toggle panel along with the plastic cover opposite the muffle of the helicopter.

4.2. Anti-vibration design

There are three main vibration sources in the UAV helicopter: (1) the rotation of the main rotor (30.8 Hz); (2) the engine (260.5 Hz); and (3) the rotation of the tail rotor (143.4 Hz). These frequencies are estimated based on a governed motor speed at 1850 rpm. The combined vibration has a amplitude about 2g, i.e., 19.6 m/s⁻², along all of the three body axes. It has potential to introduce bias to measurement data and to cause loose-of-connection of mechanical components. For this reason, an anti-vibration design is necessary to ensure the overall onboard system working properly.

For SheLion, four wire-ropc isolators are carefully selected to realize an anti-vibration aim. They are mounted symmetrically around the CG of the onboard system (see Fig. 6), and their working features are as follows:

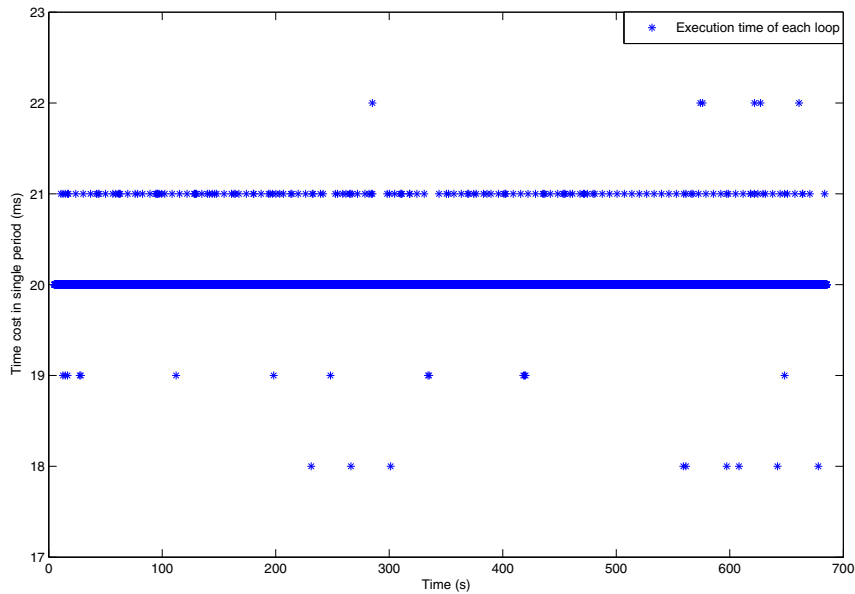


Fig. 9. Execution time of the test loops of flight control CPU.

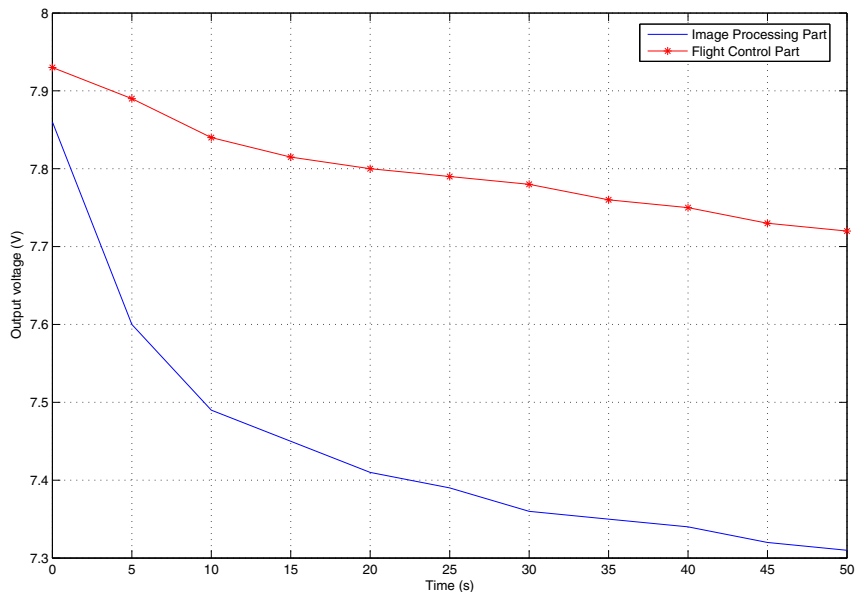


Fig. 10. Output voltages of lithium-polymer batteries.

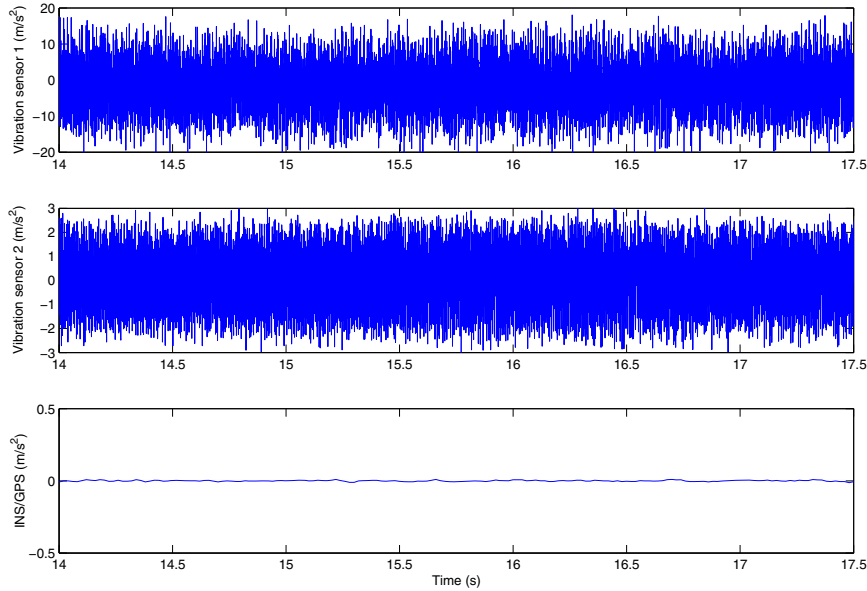


Fig. 11. Sample result of comparison of vibrational amplitude.

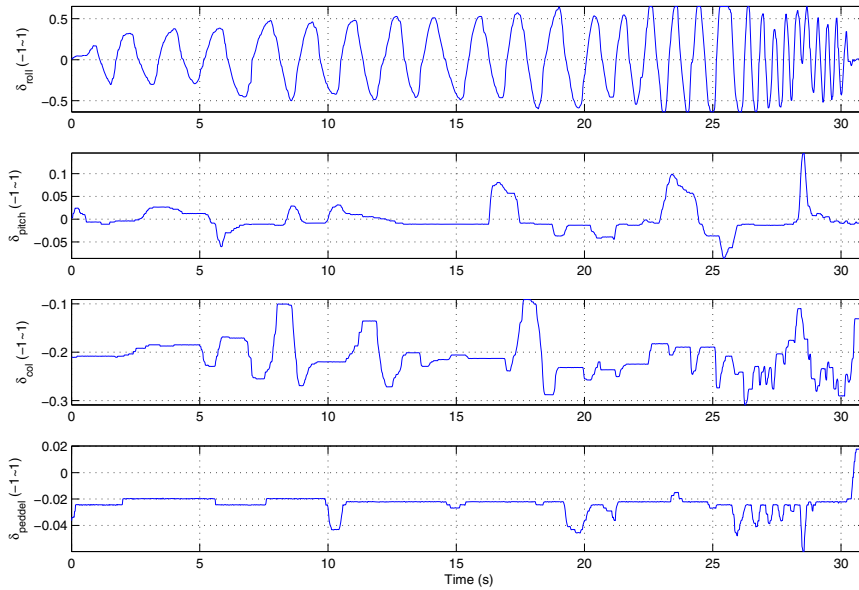


Fig. 12. Input signals in the manual flight test.

1. *45°-Compression* mounting: Such mounting method provides the same stiffness in both the horizontal and vertical directions.
2. *Good transmitting rate*: The transmitting rate is defined as the ratio of the output vibration level to the input vibration level. According to the selection rules provided by the manufacturer (see Fig. 7 for the characteristic of the wire-rope isolators), we choose a natural frequency and a cutoff frequency around 9.5 and 13.4 Hz, respectively, which are sufficient to ensure that a satisfactory transmitting rate for the vibration source with the lowest frequency, i.e., 30.8 Hz. More specifically, about 80% of the vibration at this frequency is suppressed.

Such an anti-vibration design has demonstrated to effectively reduce the harmful raw vibration and increase the overall safety. Its actual performance is to be further examined in Section 5.

4.3. Power supply design

The main consideration in the power supply design is to meet the overall experimental requirement and overall system safety. Based on the detailed power consumptions of the hardware components onboard given in Table 1 and the consideration of safety issues, we come out with a power supply scheme for SheLion, which is shown in Fig. 8, in which batteries 1 and 2 with an output voltage of 4.8 V, a power capacity of 17.5 W h and a weight of 90 g, are used to power the onboard servos and servo controllers. Although a single battery is sufficient to power the components onboard, we have chosen to use two batteries instead to enhance the overall safety of the system. The system can still run smoothly and guarantee manual maneuvering even if one of the batteries is out of order. Another feature of our design is to include the servo

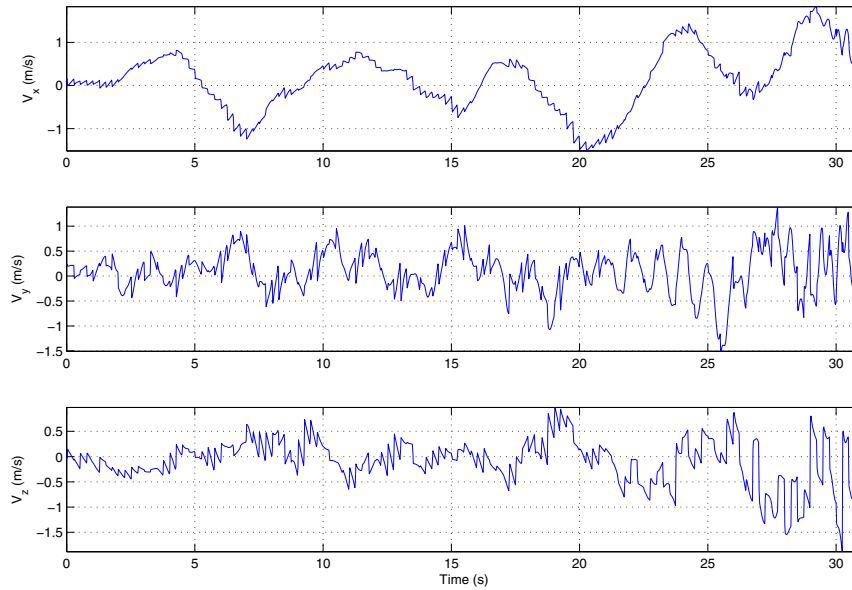


Fig. 13. Velocity outputs in the manual flight test.

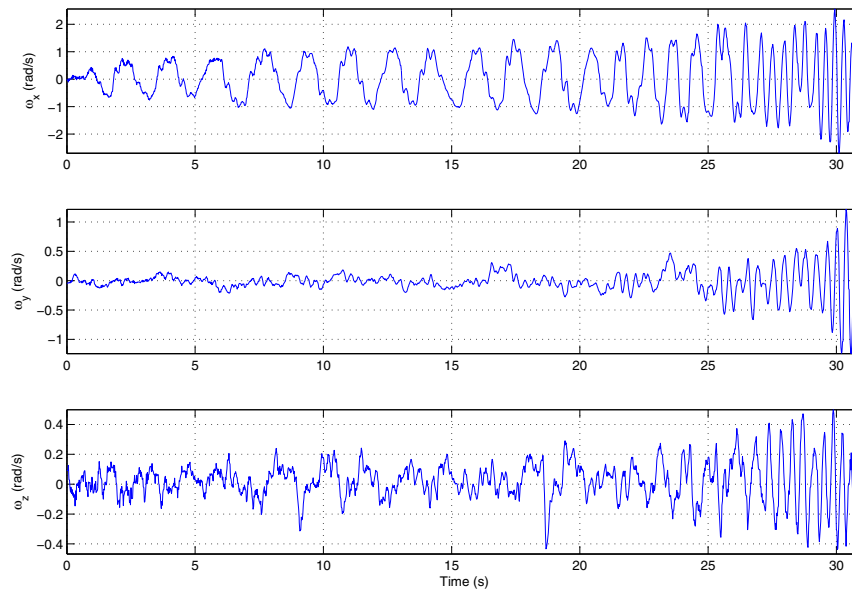


Fig. 14. Angular rates in the manual flight test.

controller with the RC helicopter as its function is extremely important for both manual and automatic flight. With such a configuration, the servo controller can still work during unexpected events, such as the breakdown of the onboard system, so that the ground pilot would still have chances to guide the helicopter.

To avoid the potential conflict of the power supply between the flight control CPU and the image processing CPU, two separate batteries (batteries 3 and 4) are used to provide power supply to these two units. To accommodate for the different input voltage levels of each individual hardware components, two high-efficiency DC-to-DC converters with a transferring rate of 92% are used to convert the output voltages of batteries 3 and 4 to 5 V and 12 V, respectively. It can be observed from Table 4 that the total power consumptions of these two groups are quite similar. We thus select two identical batteries with an output voltage of 8.4 V, a power capacity of 35 W h and a weight of 190 g, for batteries 3 and 4.

4.4. EMI shielding design

Electromagnetic interference is a serious issue for small-scaled UAV helicopters as all of the highly integrated electronic components are required to be mounted in a very limited space. The main problems aroused by EMI include: (1) reducing the effective range of RC manual control; (2) generating errors in INS/GPS measurements; and (3) causing data losses in wireless communications. These problems have to be eliminated or reduced to minimum before conducting actual flight tests. In *SheLion*, we use aluminum boxes and foil to isolate the necessary electronic components. More specifically, the key hardware components such as the servo controller board, RC receiver, MNAV100CA and wireless modem are kept in separate aluminum boxes, and the onboard system is protected with aluminum foil. As a result, we have successfully maintained the original manual control range (50 m without

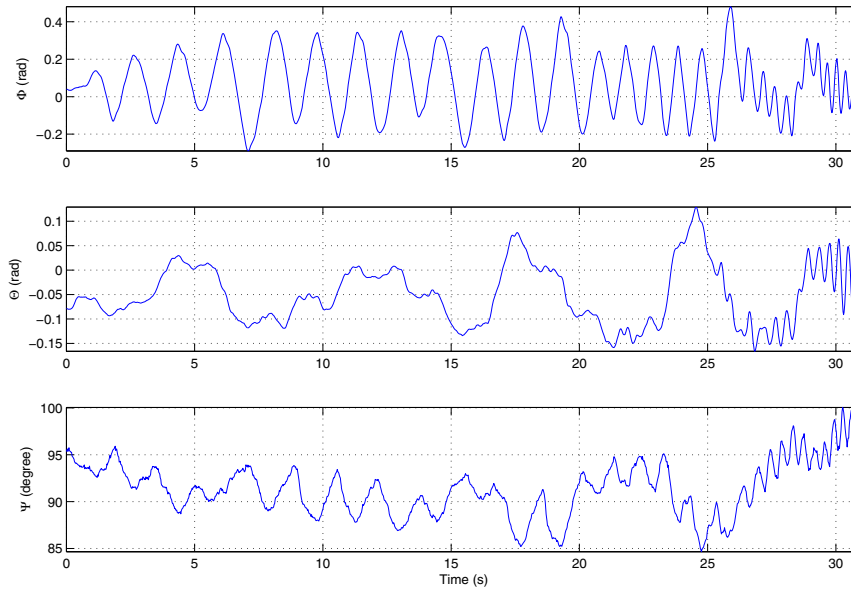


Fig. 15. Euler angles in the manual flight test.

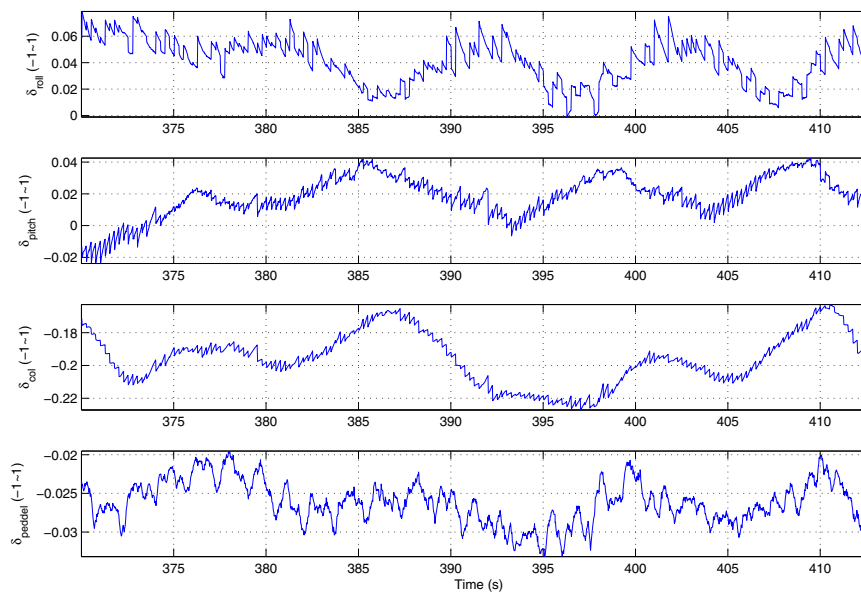


Fig. 16. Input signals in the automatic hovering flight test.

extending the antenna of the joystick), and the reliability of the MNAV100CA and wireless modem.

5. Experimental tests and evaluations

In this section, we present a series of ground tests and actual flight tests conducted to evaluate the performance and reliability of the overall UAV helicopter. These experiments show that the constructed UAV yields excellent performances in all categories.

5.1. Ground tests

During the ground tests, SheLion is placed on a level ground with its engine running at 85% of the hovering RPM, which is set to be 1850 for SheLion. The ground supporting system is placed

about 500 m away from SheLion. Each ground test lasts more than 12 min. More specifically, the following items are thoroughly examined:

1. *Flight control CPU.* For the flight control CPU, we run the onboard software system of [5] to execute iteratively all of the tasks listed in Section 3.2. We set the execution time for each iteration loop to be 20 ms, which coincides with the sampling rate of the INS/GPS. Fig. 9 shows the actual CPU execution time of all the loops tested. Clearly, the actual time consumption of each loop is in the neighborhood of 20 ms. The bias is mainly caused by the inaccuracy of the internal clock of the PC-104 ATHENA processor.
2. *Wireless communication system.* The wireless communication system between SheLion and the ground supporting system is

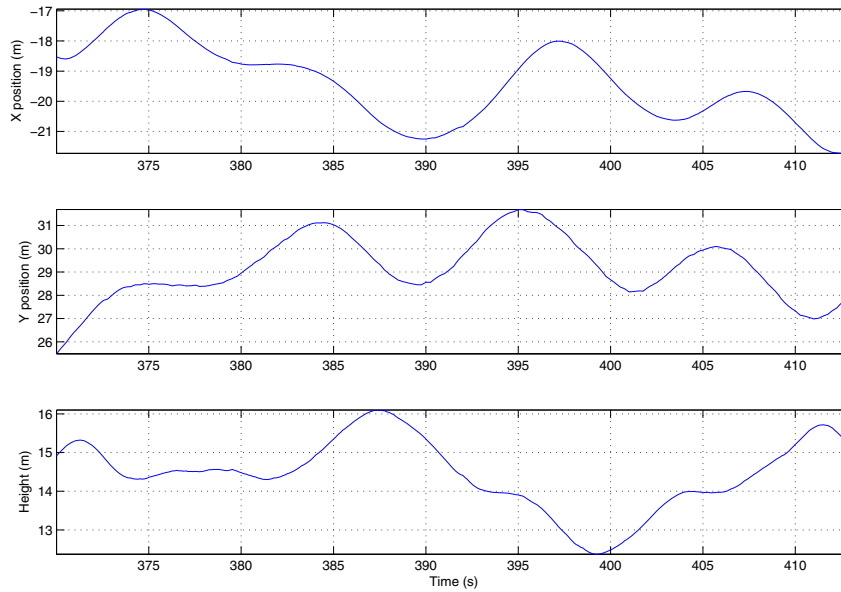


Fig. 17. Position outputs in the automatic hovering flight test.

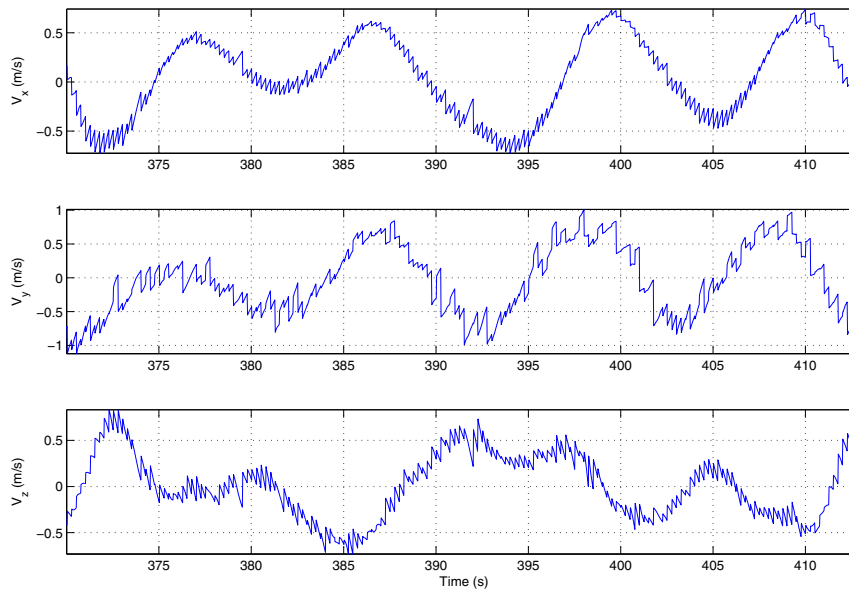


Fig. 18. Velocity outputs in the automatic hovering flight test.

tested through transmitting some pre-set data. Our test shows that the communication channel between the ground station and the UAV is perfect.

3. *Power consumption.* For this item, a special ground test which lasts 50 min is performed. The input voltages for both the flight control unit and the image processing unit are recorded periodically with a time interval of 5 min. The resulting output voltages of the batteries are plotted in Fig. 10. As expected, the output voltages of both units drop but with the reasonable slopes. The final values stay, respectively, at 7.72 V for the flight control part and 7.31 V for the image processing part, which are within the safety level for the overall system. This result indicates that the selected batteries have sufficient power to continuously supply the overall onboard system during the whole experimental period.
4. *Anti-vibration system.* To examine the efficiency of the anti-vibration system, two small-size vibration detecting sensors are used, of which one (vibration sensor 1) is stucked on a lever

of the landing skit and the other (vibration sensor 2) is attached underneath the aluminum plate of the onboard system. Fig. 11 shows a test sample of the z-axis acceleration measured by the two sensors and the measured acceleration data of the INS/GPS. With the wire-rope isolators, the resulting vibration transmitting rate is in the range of 20–25%, which indicates that our anti-vibration design is successful. Similar results are also obtained for the other two axes. We note that the remaining 20–25% vibration can be further eliminated through using the Bessel filters.

5.2. Flight tests

After successfully completing the ground tests, we next move on to test the overall UAV system in the sky under both the manual control mode and automatic control mode. For manual mode, we have conducted a series of perturbation tests. More specially,

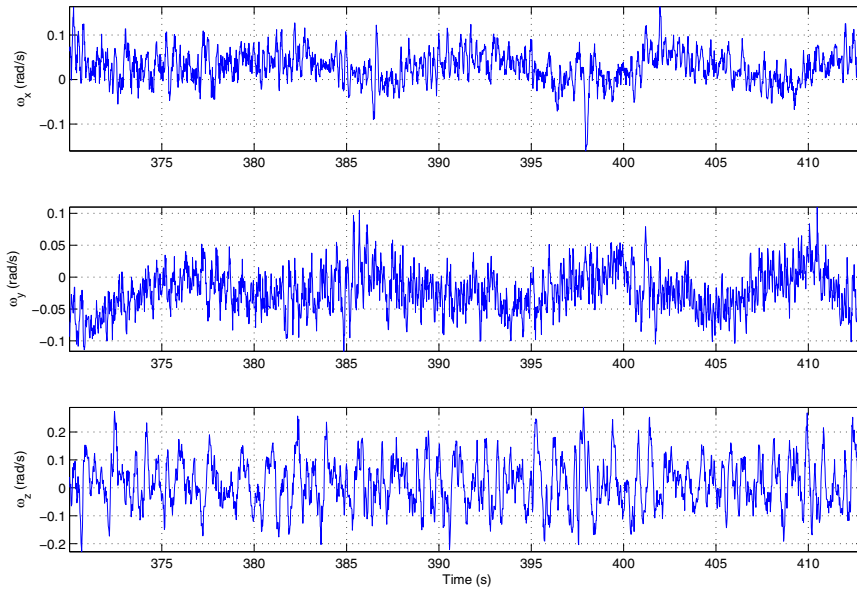


Fig. 19. Angular rates in the automatic hovering flight test.

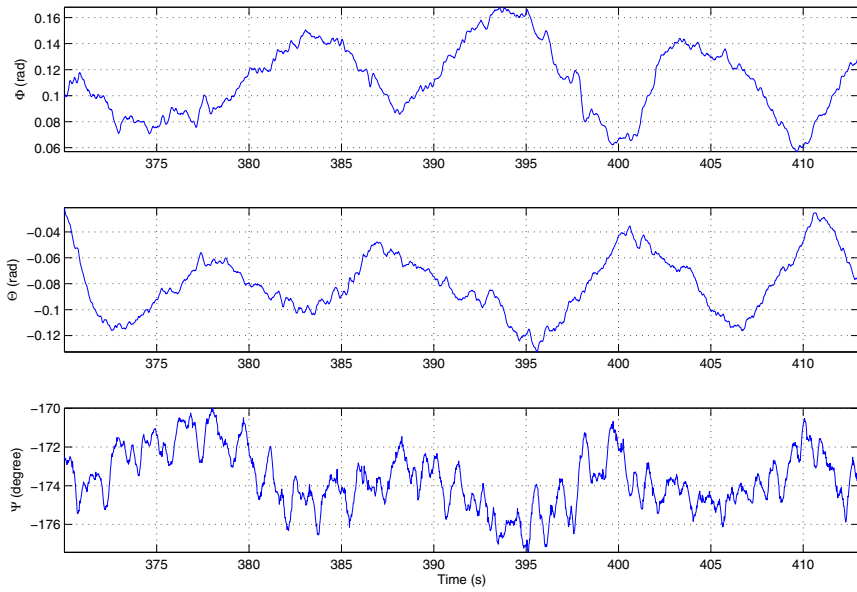


Fig. 20. Euler angles in the automatic hovering flight test.

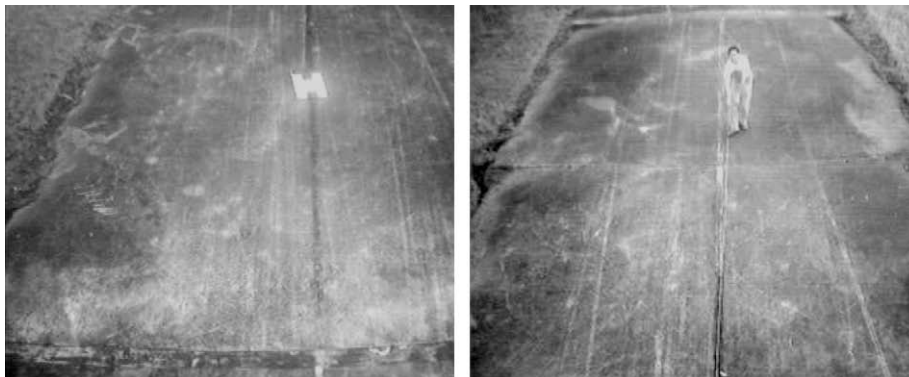


Fig. 21. Samples of ground images captured by SheLion.

we first command SheLion to be stabilized at a hovering flight condition and then inject a frequency-sweep signal to the input channels to produce perturbations up to $\pm 30^\circ$ in rolling, pitching and yawing angles, respectively. The main aim for this kind of tests is to evaluate the performance and feasibility of the UAV hardware components in drastic flight actions. Figs. 12–15 show the resulting manual flight test results. It is proved that the constructed UAV helicopter and its onboard hardware as well as software systems have been working properly in such a severe flight condition.

Automatic hovering flight is used to test the automatic mode of the integrated UAV system. After manual hovering is achieved, SheLion is commanded to switch to the automatic mode and its onboard system takes over as the control authority to continue performing the hovering flight test. The results shown in Figs. 16–20 are obtained from an automatic hovering test, which clearly indicate that SheLion is capable of hovering stably around the desired position (–19.5, 30, 14.5 m) without drifting. The constructed UAV helicopter can thus be further utilized for other developments.

In the flight test, we have also activated the image processing unit and commanded the system to capture ground images when the UAV is hovering steadily. Fig. 21 shows a pair of images captured during this process. Our post-flight examination on the mechanical components of the UAV and the data obtained clearly indicates that SheLion is very reliable in all categories tested. Finally, we refer interested readers to a video clip captured during the above mentioned flight tests at the web link: <http://hdd.ece.nus.edu.sg/~uav/wmv/shelion.wmv>.

6. Conclusions

We have presented the complete and systematic design procedure for constructing small-scale UAV helicopters, which include the hardware selection, the design and integration, and the actual ground and flight tests. Our result shows that the proposed methodology is efficient and effective. It has been successfully verified and demonstrated through the actual construction and implementation of a UAV helicopter built by our group at the National University of Singapore. The constructed UAV can be used as an excellent platform for future research development. The group is currently undergoing in obtaining a complete nonlinear dynamic model of the UAV and designing an automatic flight control system using newly developed advanced control techniques.

References

- [1] Cai G, Peng K, Chen BM, Lee TH. Design and assembling of a UAV helicopter system. In: Proceedings of 5th international conference on control and automation, Budapest, Hungary; 2005. p. 697–702.
- [2] Cai G, Chen BM, Peng K, Dong M, Lee TH. Modeling and control system design for a UAV helicopter. In: Proceedings of 14th Mediterranean conference on control and automation, Ancona, Italy; 2006. p. 600–6.
- [3] Corke P. An inertial and visual sensing system for a small autonomous helicopter. *J Robotic Syst* 2004;21:43–51.
- [4] Dittrich JS, Johnson EN. Multi-sensor navigation system for an autonomous helicopter. In: Proceedings of 21st digital avionics systems conference, Irvine, California, USA; 2002. p. 8C1.1–19.
- [5] Dong M, Chen BM, Cai G, Peng K. Development of a real-time onboard and ground station software system for a UAV helicopter. *J Aerospace Comput Inform Commun* 2007;4:933–55.
- [6] Gavrillets V, Shterenberg A, Dahleh MA, Feron E. Avionics system for a small unmanned helicopter performing aggressive maneuvers. In: Proceedings of 19th digital avionics systems conference, Philadelphia, USA; 2000. p. 1E2/1–7.
- [7] Harris C, editor. Shock and vibration handbook. New York: McGraw-Hill; 1996.
- [8] Jang JS, Liccardo D. Small UAV automation using MEMS. *IEEE Aerospace Electron Syst Mag* 2007;22:30–4.
- [9] Johnson EN, Kannan SK. Adaptive trajectory control for autonomous helicopters. *AIAA J Guidance Control Dyn* 2005;28:524–38.
- [10] LaCivita M, Messner WC, Kanade T. Modeling of small-scale helicopters with integrated first-principles and system-identification techniques. In: Proceedings of 58th forum of American helicopter society, Montreal, Canada; 2002. p. 2505–16.
- [11] Lin F, Chen BM, Lum KY. Integration and implementation of a low-cost and vision UAV tracking system. In: Proceedings of 26th Chinese control conference, Zhangjiajie, China; 2007. p. 731–6.
- [12] Mejias L, Saripalli S, Campoy P, Sukhatme GS. Visual servoing of an autonomous helicopter in urban areas using feature tracking. *J Field Robotics* 2006;23:185–99.
- [13] Mettler B. Identification modeling and characteristics of miniature rotorcraft. Norwell, MA: Norwell (MA): Kluwer Academic Publishers; 2003.
- [14] Musial M, Brandenburg UM, Hommel G. Inexpensive system design: The flying robot MARVIN. In: Proceedings of 6th international UAVs conference on unmanned air vehicle systems, Bristol, UK; 2001. p. 23.1–12.
- [15] Ollero A, Merino L. Control and perception techniques for aerial robotics. *Annu Rev Control* 2004;28:167–78.
- [16] Peng K, Dong M, Chen BM, Cai G, Lum KY, Lee TH. Design and implementation of a fully autonomous flight control system for a UAV helicopter. In: Proceedings of 26th Chinese control conference, Zhangjiajie, China; 2007. p. 662–7.
- [17] Saripalli S, Montgomery JF, Sukhatme GS. Visually-guided landing of an unmanned aerial vehicle. *IEEE Trans Robotics Automat* 2003;19:371–80.
- [18] Sharp CS, Shakenia O, Sastry S. A vision system for landing an unmanned aerial vehicle. In: Proceedings of IEEE international conference on robotics and automation, Seoul, Korea; 2001. p. 1720–7.
- [19] Shim DH, Kim HJ, Sastry S. Control system design for rotorcraft-based unmanned aerial vehicle using time-domain system identification. In: Proceedings of IEEE conference on control applications, Anchorage, Alaska, USA; 2000. p. 808–13.
- [20] Sugeno M, Hirano I, Nakamura S, Kotsu S. Development of an intelligent unmanned helicopter. In: Proceedings of IEEE international conference on fuzzy systems, Yokohama, Japan; 1995. p. 33–4.
- [21] Tischler MB, Rempel RK. Aircraft and rotorcraft system identification – engineering methods with flight test examples. Reston, VA: AIAA; 2006.
- [22] Velez CM, Agudelo A, Alvarez J. Modeling, simulation and rapid prototyping of an unmanned mini-helicopter. In: Proceedings of AIAA modeling and simulation technologies conference and exhibit, Keystone, Colorado; 2006. p. AIAA-2006-6737.
- [23] Yun B, Peng K, Chen BM. Enhancement of GPS signals for automatic control of a UAV helicopter system. In: Proceedings of IEEE international conference on control and automation, Guangzhou, China; 2007. p. 1185–9.